Thailand Statistician
October 2022; 20(4): 905-917
http://statassoc.or.th
Contributed paper

Circular Generalized Logistic Distributions and its Applications

Sakthivel Kandasamy Maruthan*[a], and Alshad Karippayil Bava [b]
[a] Department of Statistics, Bharathiar University, Coimbatore, Tamil Nadu, India.
[b] Sri Ramachandra Faculty of Engineering and Technology, Sri Ramachandra Institute of Higher Education and Research, Chennai, Tamil Nadu, India.
*Corresponding author; e-mail: sakthithebest@gmail.com

Received: 5 October 2020
Revised: 21 January 2021
Accepted: 24 January 2021

Abstract

This paper introduces three circular distributions based on inverse stereographic projection by considering three types of logistic distribution available in the literature, namely Type-I generalized logistic distribution, three parameter Type-I generalized logistic distribution and Type-II generalized logistic distribution. The proposed new models are more flexible than stereographic logistic model (DattatreyaRao et al. 2016) to the optimal modeling of circular data, can take skewness and heavy tails into account and offer a great applicability in many fields. Since one of the proposed models called circular Type-II generalized logistic distribution shows more applicability than the other proposed models. Hence, in this paper we discuss the method maximum likelihood estimation and a simulation study for circular type–II generalized logistic distribution. Finally, four circular data-sets are considered for illustrative purposes and proving that the proposed models perform well than several other circular distributions.

Keywords: Circular data, inverse stereographic projection, simulation study.

1. Introduction

During the last few decades, circular distributions have been showed of significant interest both in terms of their methodological improvement as well as practical applications. This is due to the analysis of circular data is little complicated than the analysis of linear data, this is mainly because, the restriction of the support of the data on the unit circle is $[0,2\pi)$ or $[-\pi,\pi)$. Several authors have extensively studied circular modeling in different kinds of practical problems. The direct applications of circular models can be seen mostly in biology, medicine, geology, astronomy and meteorology. There are many ways to derive a circular distribution; one of them is inverse stereographic projection proposed by Minh and Farnum (2003). This can be defined as follows.

Let X be a random variable with density function $f(x)$ and distribution function $F(x)$ respectively. Let $g(\theta)$ and $G(\theta)$ be the density function and distribution function of the random

point on the unit circle respectively. Then, $g(\theta)$ and $G(\theta)$ can be written in terms of $f(x)$ and $F(x)$, involving two parameters u and v is given by

$$g(\theta)=\frac{v}{2}\left(1+\tan^2\left(\frac{\theta}{2}\right)\right)f\left(u+v\tan\left(\frac{\theta}{2}\right)\right), \tag{1}$$

$$G(\theta)=F\left(u+v\tan\left(\frac{\theta}{2}\right)\right)=F\left(T(\theta)\right). \tag{2}$$

Rest of this paper, we will assume that $v>0$ and $u=1$. In recent years, a lot of distributions have been introduced using ISP method. To list a few, DattatreyaRao et al. (2016) introduced a circular model by applying the ISP on the Logistic model and discussed its applicability on 50 noisy scrub birds' data set. Abuzaid (2017) and Rambli et al. (2019) introduced half-circular Burr-XII and half-circular transformed Gamma distribution respectively using ISP to analyze posterior corneal curvature. Subrahmanyam et al. (2017) proposed a new family of circular distributions called Semicircular new Weibull Pareto distribution. Sreekanth et al. (2018) discussed Stereographic l-axial half logistic distribution and some of its properties. Recently, Srinivas et al. (2019) derived semicircular extreme-value distribution over a semicircular segment.

The logistic distribution is well known in statistics and very useful in a wide variety of applications, especially in, sports modeling, finance and physical sciences. The simplicity and applicability of logistic distribution have made it one of the most important statistical distributions in Statistics. In this paper, we consider the three circular distributions called circular Type-I generalized logistic (CGL-I) distribution, two-parameter Type-I logistic (CTGL-I) distribution and circular Type-II generalized logistic (CGL-II)distribution, based on inverse stereo graphic projection by considering three type of logistic distribution available in the literature, namely Type-I generalized logistic distribution, three-parameter Type-I generalized logistic distribution and Type-II generalized logistic distribution and we give a consideration to the study the circular Type-II generalized logistic distribution and moreover we investigate the flexibility and applicability of the new proposed circular models using four real circular data sets. The rest of the paper is structured as follows: in Section 2, we discuss three types of generalized logistic distribution. In Section 3, we introduce the new circular models and present graphs of PDF for various values of parameters. Section 4 discusses the method of maximum likelihood estimation and a simulation study of the CGL-II model. In Section 5, we consider four real data sets to show the applicability of new models. Finally, in Section 5, work is concluded.

2. Generalized Logistic Distributions on the Real Line

There are many generalizations of logistic distribution which were proposed by different researchers. We mainly consider three different generalizations of the logistic distribution; the first generalization is known as the Type-I generalized logistic (GL-I) distribution proposed by Ahuja and Nash (1967) and Gupta and Kundu (2010) utilized even more better sense and they viewed this model as a proportional reversed hazard distribution called it as proportional reversed hazard logistic distribution used to model both left and right skewed data and studied its several properties. Secondly, we consider an extension of GL-I distribution studied by Gupta and Kundu (2010) and finally, we will discuss Type-II generalized logistic distribution see for more details, Johnson, et al, (1995). The PDF and CDF of these distributions are given in the following section.

2.1. Type-I generalized logistic distribution

The Type-I generalized logistic (GL-I) distribution is an attractive generalization of the logistic distribution, contains one parameter and is defined as follow.

Let X follows one parameter GL-I distribution then the PDF and CDF of X is given by

$$g_1(x) = \frac{\alpha e^{-x}}{\left(1+e^{-x}\right)^{(\alpha+1)}}, \tag{3}$$

$$G_1(x) = \frac{1}{\left(1+e^{-x}\right)^{\alpha}}, \tag{4}$$

where $-\infty < x < \infty,\ \alpha > 0$ and the distribution is negatively skewed for $0 < \alpha < 1$ and positively skewed for $\alpha > 1$. Gupta and Kundu (2010) introduced location parameter $-\infty < \mu < \infty$ and scale parameter $\lambda > 0$ in (1) as follows

$$g_2(x) = \frac{\alpha\lambda e^{-\lambda(x-\mu)}}{\left(1+e^{-\lambda(x-\mu)}\right)^{(\alpha+1)}}, \tag{5}$$

$$G_2(x) = \frac{1}{\left(1+e^{-\lambda(x-\mu)}\right)^{\alpha}}, \tag{6}$$

where $-\infty < x < \infty,$ proportionality parameter $\alpha > 0,$ location parameter $\mu > 0$ and scale parameter $\lambda > 0.$ We referred it as three parameter Type-I generalized logistic distribution and it is abbreviated as TGL-I.

2.2. Type-II generalized logistic distribution

The PDF and CDF of Type-II generalized logistic (GL-II) distribution are respectively given by

$$g_3(x) = \frac{\alpha e^{-\alpha x}}{\left(1+e^{-x}\right)^{(\alpha+1)}}, \tag{7}$$

$$G_3(x) = 1 - \frac{e^{-\alpha x}}{\left(1+e^{-x}\right)^{\alpha}}, \tag{8}$$

where $-\infty < x < \infty$ and $\alpha > 0.$ Note that if X has a Type-I generalized distribution in (3), then $-X$ has a Type-II generalized distribution. Therefore, the GL-II distribution defined in (7) is positively skewed for $0 < \alpha < 1$ and negatively skewed for $\alpha > 1.$

3. Circular Generalized Logistic Distribution

In this section, we apply inverse stereographic projection method to the above mentioned three different logistic distributions. The functional relation of ISP involving two parameters u and v is given in Equation (1) and (2). Now we will obtain three different circular generalized logistic distributions in the following three subsections.

3.1. Circular Type-I generalized logistic distribution

Considering the inverse stereographic projection on the Type-I generalized logistic distribution (3), the corresponding circular PDF and CDF of circular Type-I generalized logistic distribution (CGL-I) are given as

$$g_1(\theta)=\frac{\alpha v\sec^2\left(\theta/2\right)}{2\left(1+e^{-\left(1+v\tan\left(\theta/2\right)\right)}\right)^{\alpha}\left(1+e^{\left(1+v\tan\left(\theta/2\right)\right)}\right)}, \tag{9}$$

$$G_1(\theta)=\frac{1}{\left(1+e^{-\left(\left(1+v\tan\left(\theta/2\right)\right)\right)}\right)^{\alpha}}, \tag{10}$$

where $-\pi<\theta<\pi,$ location parameter $\alpha>0$ and scale parameter $v>0.$

Now, we applying the inverse stereographic projection on the second generalization of logistic distribution defined in (5), then the PDF and CDF of the circular two-parameter Type-I logistic (CTGL-I) distribution are obtained as

$$g_2(\theta)=\frac{\alpha\lambda v\sec^2\left(\theta/2\right)}{2\left(1+e^{-\lambda\left(1+v\tan\left(\theta/2\right)-\mu\right)}\right)^{\alpha}\left(1+e^{\lambda\left(1+v\tan\left(\theta/2\right)-\mu\right)}\right)}, \tag{11}$$

$$G_2(\theta)=\frac{1}{\left(1+e^{-\lambda\left(\left(1+v\tan\left(\theta/2\right)\right)-\mu\right)}\right)^{\alpha}}, \tag{12}$$

where $-\pi<\theta<\pi,$ proportionality parameter $\alpha>0,$ location parameter $\mu>0$ and scale parameters $\lambda>0$ and $v>0.$

3.2. Circular Type-II generalized logistic distribution

The PDF and CDF of the circular Type-II generalized logistic distribution (CGL-II) can be obtained by using the inverse stereographic projection and are given by respectively,

$$g_3(\theta)=\frac{\alpha v\sec^2\left(\theta/2\right)e^{-\alpha\left(1+v\tan\left(\theta/2\right)\right)}}{2\left(1+e^{-\left(1+v\tan\left(\theta/2\right)\right)}\right)^{\alpha+1}}, \tag{13}$$

$$G_3(\theta)=1-\frac{e^{-\alpha\left(1+v\tan\left(\theta/2\right)\right)}}{\left(1+e^{-\left(1+v\tan\left(\theta/2\right)\right)}\right)^{\alpha}}, \tag{14}$$

where $-\pi<\theta<\pi,$ location parameter $\alpha>0$ and scale parameter $v>0.$

In order to show the flexibility and behavior of each distributions derived above, we displayed the density plot (see Figures 1-3) for various parameter values and the confirms that the proposed models are very flexible and shows various shapes.

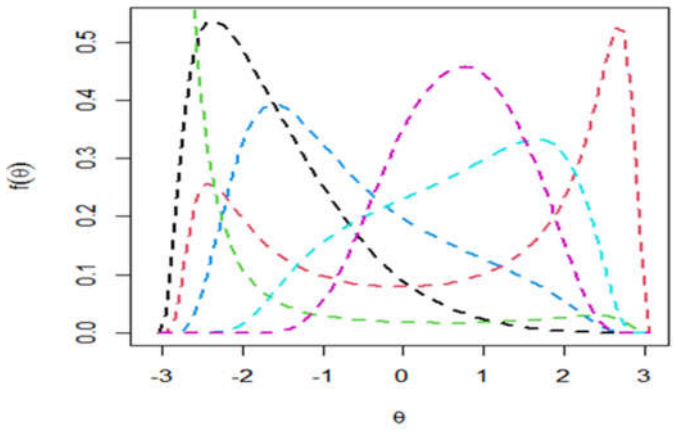

---- $\alpha = 0.2, v = 3.5$ ---- $\alpha = 5, v = 6$ ---- $\alpha = 6, v = 6.5$
---- $\alpha = 3, v = 16$ ---- $\alpha = 7, v = 20$ ---- $\alpha = 1, v = 20$

Figure 1 Density function plots of CGL-I distribution

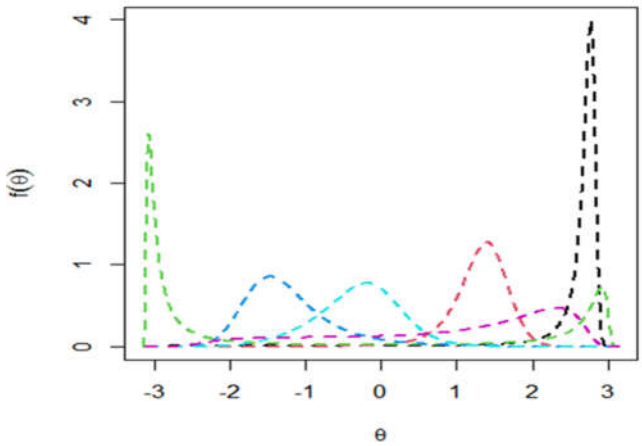

--- $\alpha = 0.5, \mu = 3, \lambda = 3.7, v = 0.5$ --- $\alpha = 1.2, \mu = 2.2, \lambda = 3, v = 2.6$
--- $\alpha = 0.2, \mu = 0.5, \lambda = 5, v = 0.6$ --- $\alpha = 1, \mu = 4, \lambda = 0.22, v = 1$
--- $\alpha = 0.5, \mu = 2, \lambda = 1, v = 4$ --- $\alpha = 2, \mu = 2.5, \lambda = 1, v = 0.4$

Figure 2 Density function plots of CTGL-I distribution

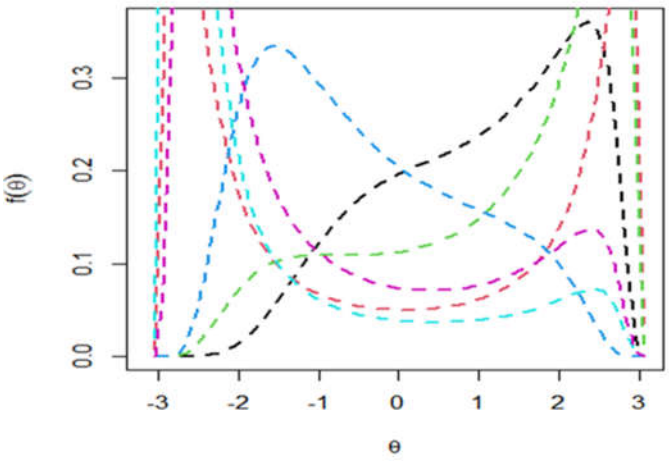

--- $\alpha = 0.2, v = 3.5$ --- $\alpha = 0.6, v = 0.5$ --- $\alpha = 0.2, v = 2$
--- $\alpha = 0.8, v = 2$ --- $\alpha = 1.5, v = 0.5$ --- $\alpha = 1, v = 0.75$

Figure 3 Density function plots of CGL-II distribution

4. Quantile Function, Estimation and Simulation Study of CGL-II Distribution

In this section, we derive the quantile function, ML estimators and present a simulation study for CGL-II distribution.

4.1. Quantile function

By inverting the CDF defined in Equation (14), we obtain the quantile function of the CGL-II distribution as

$$\theta_q = F^{-1}(u) = Q(u) = 2\tan^{-1}\left(\frac{1-\log\left(\frac{1}{u^{1/\alpha}}-1\right)}{-v}\right). \tag{15}$$

4.2. Maximum likelihood estimation

Here, we discuss the method of maximum likelihood estimation to estimate the parameters of CGL-II distribution. Suppose the random sample $\theta_1, \theta_2, \ldots, \theta_n$ of size n is drawn from CGL-II distribution with PDF $f(\theta;\alpha,\beta,\lambda,v)$, then the log-likelihood function is given by

$$\log L = n\log\left(\frac{\alpha v}{2}\right) + \sum_{i=1}^{n}\log\left(\sec^2\left(\theta_i/2\right)\right) - \sum_{i=1}^{n}\log\, e^{\left(1+v\tan\left(\theta_i/2\right)\right)} - (\alpha+1)\sum_{i=1}^{n}\log\left(1+e^{-\left(1+v\tan\left(\theta_i/2\right)\right)}\right). \tag{16}$$

Differentiating Equation (14) with respect to α and v and equating to zero gives

$$\frac{\partial \log L}{\partial \alpha} = \frac{n}{\alpha} - v\tan\left(\theta_i/2\right) + 1 - \sum_{i=1}^{n}\log\left(1+e^{-\left(1+v\tan\left(\theta_i/2\right)\right)}\right) = 0, \tag{17}$$

$$\frac{\partial \log L}{\partial v} = \frac{n}{v} - \alpha\tan\left(\theta_i/2\right) - \frac{(\alpha+1)\tan\left(\theta_i/2\right)}{\left(1+e^{\left(1+v\tan\left(\theta_i/2\right)\right)}\right)} = 0. \tag{18}$$

Since the equations (17) and (18) cannot be determined analytically, some numerical methods like Newton-Raphson algorithm is to be employed to get a solution for parameters.

4.3. Simulation study

In this section, we present a simulation study to evaluate the performance of the maximum likelihood estimators obtained in the previous section by drawing different samples sizes (n = 30, 50, 100, 200) from the CGL-II distribution for the combination of fixed parameter values $\alpha = 0.9, 1.5$ and $\lambda = 0.5, 0.8$. The values of parameter are to be estimated and computed the corresponding bias and mean square errors (MSE) for each sample size and the results are displayed in Table 1. The following algorithm is used for this study.

(i) Generate the values of u_i ~ uniform(0, 1) for $i = 1, 2, 3, ..., n$; (n = 30, 50, 100, 200).

(ii) Set $\theta_i = F^{-1}(u_i)$ and now θ_i follows CGL distribution, where $F^{-1}(.)$ is the quantile function provided in (15).

(iii) Calculate the MLE estimates of the parameters of the CGL distribution using the values of θ's.

(iv) Repeat Steps (i) to (iii) in for 1,000 times (Since replication $N = 1,000$)

(v) Calculate the bias and MSE for the replication 1,000 estimates and for each value of n.

Table 1 Average biases and MSEs of the simulated estimates

		$\alpha = 0.9$				$\alpha = 1.5$			
		$\hat{\alpha}$		$\hat{\lambda}$		$\hat{\alpha}$		$\hat{\lambda}$	
n		Bias	MSE	Bias	MSE	Bias	MSE	Bias	MSE
$\lambda = 0.5$	30	0.0186	0.0396	0.0329	0.0100	0.0432	0.0909	0.0261	0.0071
	50	0.0108	0.0234	0.0161	0.0055	0.0219	0.0528	0.0118	0.0039
	100	0.0025	0.0104	0.0094	0.0025	0.0166	0.0248	0.0084	0.0018
	200	0.0019	0.0053	0.0042	0.0011	0.0081	0.0121	0.0009	0.0009
$\lambda = 0.8$	30	0.0158	0.0409	0.0431	0.0276	0.0531	0.1117	0.0371	0.0201
	50	0.0080	0.0215	0.0247	0.0138	0.0253	0.0479	0.0176	0.0108
	100	0.0094	0.0110	0.0126	0.0063	0.0168	0.0256	0.0106	0.0049
	200	0.0020	0.0054	0.0046	0.0030	0.0047	0.0127	0.0054	0.0025

The result of simulation study shows that the maximum likelihood estimators of CGL-II model are precise and accurate. Since the values of bias and mean square error (MSE) of the parameter estimates decrease to zero as sample size increases.

5. Applications

In this section, four real angular data sets are considered to demonstrate the flexibility and applicability of the circular generalized logistic distributions. For the data sets, MLEs of the model parameters are calculated and the model selection is accomplished using negative log-likelihood function, Akaike information criterion (AIC), consistent Akaike information criterion (CAIC), Bayesian information criterion (BIC), and the Hannan-Quinn information criterion (HQIC).

5.1. Eye data set

Consider an eye data set obtained from a glaucoma clinic at the University of Malaya Medical Centre, Malaysia. Images of the posterior segment of the eyes of 23 patients were taken using the Anterior Segment Optical Coherence Tomography (AS-OCT). Recently, Rambli et al. (2019) and Abuzaid (2017) conducted an analysis on this data as an application of the half-circular transformed gamma distribution and half-circular Burr-XII distribution respectively. The data set displayed in Table 2 and Figure 4 shows the corresponding rose diagram.

Table 2 Eye data set

1.60	1.21	1.46	2.10	1.40	1.82	1.57	1.56	1.85	0.60	1.70	1.97
1.47	1.74	1.67	1.38	0.53	1.69	1.63	1.56	1.81	2.09	2.29	

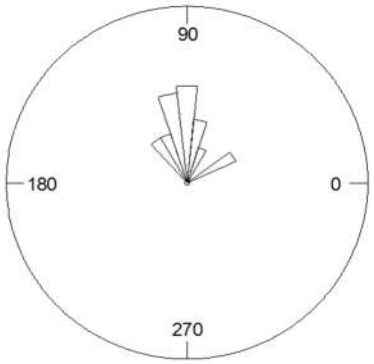

Figure 4 Rose diagram for posterior corneal curvature

For posterior corneal curvature data, we compare the fit with the following distributions: Generalized wrapped exponential (GWE) distribution (Sakthivel and Alshad, 2020), Wrapped improved second-degree Lindley (WIL) distribution, (Sakthivel and Alshad 2021), Wrapped exponential (WE) distribution (Jammalamadaka and Kozubowski 2004), wrapped Lindley (WL) distribution, (Joshi and Jose 2018), wrapped Laplace (WLa) distribution (Jammalamadaka and Kozubowski 2004), half-circular transformed gamma (Hc-T gam) distribution (Rambli et al. 2019) and half circular Burr-XII (Hc-BurrXII) distribution (Abuzaid 2017).

From Table 3, it can be observed that the values of AIC, CAIC, BIC and HQIC of the CGL-I distribution is smaller than that of the other models. This means that the CGL-I distribution better fit than other models to this data.

5.2. Homing Pigeons Data

The second data set mentioned in Batschelet (1981) and taken from Jammalamadaka and SenGupta (2001) consists of vanishing angles of 13 homing pigeons were released singly in the Toggenburg Valley in Switzerland sub Alpine conditions. They did not seem to have adjusted rapidly to the homing direction but preferred to fly in the direction of the valley. These angular observations are arranged in ascending order displayed in Table 4 and the rose diagram of the dataset shows in Figure 5.

Table 3 Goodness-of-fit statistics for eye data set

Model	Estimates	–2L	AIC	CAIC	BIC	HQIC
CGL-I	$\hat{\alpha} = 28.5999$ $\hat{v} = 2.5765$	**22.0525**	**26.05251**	**26.6525**	**28.3234**	**26.6236**
CTGL-I	$\hat{\alpha} = 0.1487$ $\hat{\lambda} = 4.0125$ $\hat{\mu} = 1.4163$ $\hat{v} = 0.3644$	19.1162	27.1163	29.3384	31.6581	28.2584
GWE	$\hat{a} = 13.7$ $\hat{\beta} = 1.964$	35.2276	39.2276	39.8276	41.4985	39.7987
WIL	$\hat{\lambda} = 1.288$	28.6824	59.3648	59.5552	60.5003	59.6504
WLind	$\hat{\lambda} = 0.913$	30.7432	63.4865	63.6769	64.6219	63.7720
WE	$\hat{\alpha} = 0.5590$	66.3914	68.3914	68.5819	69.5269	68.6770
WLa	$\hat{\alpha} = 1.095$	98.9023	100.9020	101.0920	100.0370	101.1878
Hc-BurrXII	$\hat{a} = 4.379$ $\hat{\beta} = -0.947$	242.1030	246.1030	246.8260	248.373	246.6741
Hc-T gam	$\hat{\alpha} = 5.72$ $\beta = 5.18$	642.9550	646.9550	647.6780	649.2250	647.5261

Table 4 Homing pigeons' data

20	135	145	165	170	200	300	325	335	350	350	350	355

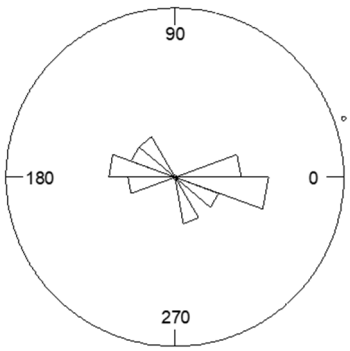

Figure 5 Rose diagram for homing pigeons' data

For Homing pigeons' data, we compare the fit with the following distributions Stereographic Logistic (SLG) distribution (DattatreyaRao et al. 2016), stereographic double exponential distribution (SDEXP), (Girija et al. 2014), Wrapped logistic distribution (WLG), (DattatreyaRao et al. 2007).

Table 5 Goodness-of-fit statistics for homing pigeons' data

Model	Estimates	–2L	AIC	CAIC	BIC	HQIC
CGL-II	$\hat{\alpha} = 0.3555$ $\hat{\nu} = 0.9145$	**52.9060**	**56.9060**	**58.1060**	**58.0358**	**56.6737**
CGL-I	$\hat{\alpha} = 2.9719$ $\hat{\nu} = 0.3896$	54.2199	58.2199	59.4199	59.3498	57.9877
SLG	$\hat{\mu} = 2.0388$ $\hat{\sigma} = 0.8278$	55.3650	59.3649	60.5649	60.4948	59.1327
SDEXP	$\hat{\mu} = -0.2735$ $\hat{\sigma} = 0.2156$	55.7537	59.7537	60.9537	60.8835	59.5214
WLG	$\hat{\mu} = -0.2735$ $\hat{\sigma} = 0.2156$	82.7950	86.7950	87.9950	87.9240	86.5620

The results in Table 5 indicate that the CGL-II distribution gives the smallest values for AIC, CAIC, BIC, and HQIC value for the Homing pigeons data set among other the fitted distributions. So, the CGL-II model could be chosen for the study.

5.3. Sea star movement data

The third dataset discussed in Fisher (1993) comprises the resultant directions of 22 sea stars, 11 days after the displacement from their natural habitat. The data set and corresponding rose diagram are given in Table 6 and Figure 6 respectively.

Table 6 Sea star movement data

1	1	3	3	8	13	16	18	30	31	43	45	147	298	329	332
335	340	350	354	356	357										

For sea star movement data, we compare the fit with the following distributions: Stereographic Logistic (SLG) distribution (DattatreyaRao et al. 2016), Generalized wrapped exponential (GWE) distribution (Sakthivel and Alshad 2020), wrapped Lindley (WL) distribution (Joshi and Jose 2018), alternative wrapped exponential (AWE) distribution, (Joshi 2016), wrapped exponential (WE) distribution (Jammalamadaka and Kozubowski 2004).

It observed from Table 7 that the values of $-2\hat{\ell}$, AIC, CAIC, BIC and HQIC of the CGL-II distribution is less than that of the values of the other models. This means that the CGL-II distribution is more applicable to fit this data.

Table 7 Goodness-of-fit statistics for sea star data

Model	Estimates	–2L	AIC	CAIC	BIC	HQIC
CGL-II	$\hat{\alpha} = 0.3622$ $\hat{v} = 7.5962$	**46.323**	**50.323**	**50.954**	**52.505**	**50.837**
CGL-I	$\hat{\alpha} = 2.8280$ $\hat{v} = 3.5299$	50.799	54.800	55.431	56.981	55.313
SLG	$\hat{\alpha} = 0.2396$ $\hat{v} = 0.0401$	55.505	59.506	60.137	61.687	60.019
GWE	$\hat{\lambda} = 0.479$ $\hat{\beta} = 00000.1$	66.179	70.180	70.811	72.361	70.693
WL	$\hat{\lambda} =$ -1.454e - 05	80.866	82.867	83.066	83.957	83.123
AWE	$\hat{\lambda} = 0.3000$	76.097	78.098	78.297	79.188	78.354
WE	$\hat{\lambda} = 0.1342$	79.585	81.586	81.785	82.672	81.842

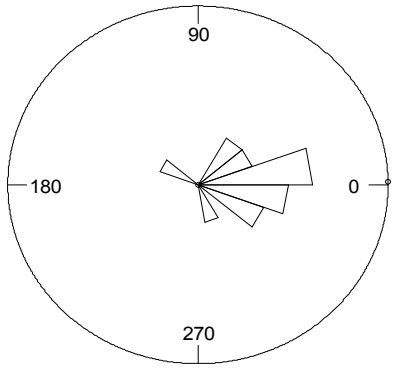

Figure 6 Rose diagram for sea star movement data

5.4. Wind data

The dataset contains 21 wind directions (see Johnson and Wehrly (1977)) by a Milwaukee weather station, at 6.00 A.M. on consecutive days. The data set and rose diagram are displayed in Table 8 and Figure 7, respectively.

Table 8 Wind directions data

356	97	211	232	343	292	157	302	335	302	324	85	324	340	157
238	254	146	232	122	329									

For wind directions data set, we compared the fit with stereographic logistic (SLG) distribution (DattatreyaRao et al. 2016) and wrapped Lindley (WL) distribution (Joshi and Jose 2018).

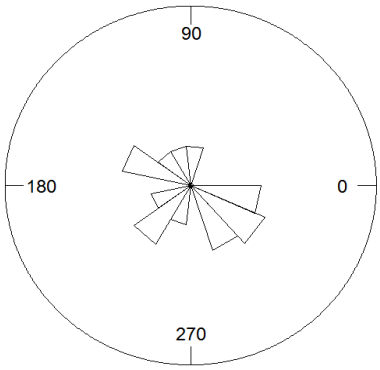

Figure 7 Rose diagram for wind directions data

Table 9 Goodness-of-fit statistics for wind directions data

Model	Estimates	$-2\hat{l}$	AIC	CAIC	BIC	HQIC
CGL-II	$\hat{\alpha} = 2.1265$ $\hat{v} = 0.7619$	73.3408	77.3408	78.0074	79.4298	77.7942
CGL-I	$\hat{\alpha} = 0.5445$ $\hat{v} = 1.2259$	73.9356	77.9356	78.6022	80.0246	78.3889
SLG	$\hat{\alpha} = 1.1112$ $\hat{v} = -0.1007$	75.6644	79.6645	80.3311	81.7534	80.1177
WL	$\hat{\lambda} = -6.17e-06$	77.1908	79.1908	79.4013	80.2353	79.4175
CTGL-I	$\hat{\alpha} = 4.457$ $\hat{v} = 1.1030$ $\hat{\mu} = 2.0333$ $\hat{\lambda} = 0.6198$	73.603	81.6030	84.103	85.7810	82.5097

From Table 9, the CGL-II distribution has the minimum log-likelihood AIC, CAIC, BIC and HQIC values compared to the other fitted models. Hence, CGL-II model provides a better fit to the wind data set compared to the other models.

6. Summary

This paper introduced three circular probability distribution namely circular Type-I generalized logistic distribution, two-parameter Type-I logistic distribution, circular Type-II generalized logistic distribution based on inverse stereographic projection which provides more flexibility in modeling asymmetric and heavy tailed circular data. The PDF plots of these proposed models for different combinations of the parameters are displayed. Further, the circular Type-II generalized logistic distribution shows good applicability, hence we have discussed the maximum likelihood estimation and a simulation study is carried out to investigate the statistical properties of the ML estimators for finite sample size. Finally, to assess the applicability of the proposed models, four real data sets have been used and its goodness-of-fit was compared with some relevant circular models.

Reference

Abuzaid AH. A half circular distribution for modeling the posterior corneal curvature. Commun Stat-Theory Methods. 2017; 47(13): 3118-3124.

Ahuja JC, Nash S. The generalized Gompertz-Verhulst family of distributions. Sankhya Ser A. 1967; 29(2): 141-156.

Batschelet, E. Circular statistics in biology, London: Academic Press; 1981.

DattatreyaRao AV, RamabhadraSarma I, Girija SVS. On wrapped version of some life testing models. Commun Stat-Theory Methods. 2007; 36(11): 2027-2035.

DattatreyaRao AV, Girija SVS, Yedlapalli P. Stereographic logistic model-application to noisy scrub birds data. Chil J Stat. 2016; 7(2): 69-79.

Fisher NI. Statistical analysis of circular data. Cambridge: Cambridge University Press; 1993.

Gupta RD, Kundu D. Generalized logistic distributions. J Appl Statist Sci. 2010; 18(1): 51-66.

Girija SVS, DattatreyaRao AV. Yedlapalli P. New Circular model induced by inverse stereographic projection on double exponential model-application to birds migration Data. J Appl Math Stat Inform. 2014; 10(1): 5-17.

Jammalamadaka SR, Kozubowski TJ. New families of wrapped distributions for modeling skew circular data. Commun Stat-Theory Methods. 2004; 33(9): 2059-2074.

Johnson NL, Kotz S, Balakrishnan N. Continuous univariate distributions. New York: John Wiley and Sons; 1995.

Johnson RA, Wehrly T. Measures and models for angular correlation and angular-linear correlation. J R Stat Soc Series B Stat Methodol. 1977; 39(2): 222-229.

Joshi S. Inference for change-points and related problems under censoring. PhD [dissertation], Rajasthan: Central University of Rajasthan; 2016.

Joshi S, Jose KK. Wrapped Lindley distribution. Commun Stat-Theory Methods. 2018; 47(5): 1013-1021.

Minh DL, Farnum NR. Using bilinear transformations to induce probability distributions. Commun Stat-Theory Methods. 2003; 32(1); 1-9.

Rambli A, Mohamed I, Shimizu K, Ramli NM. A half-circular distribution on a circle. Sains Malays. 2019; 48(4): 887-892.

Sakthivel KM, Alshad KB. A generalization of wrapped exponential distribution: properties and application. Int J Math Stat. 2020; 21 (3): 27-37.

Sakthivel KM, Alshad KB. Wrapped improved second degree Lindley distribution: properties and application. Int J Math Comput. 2021; 32 (1): 72-77.

Sreekanth Y, Yedlapalli P, Girija SVS, DattatreyaRao AV. Stereographic L-axial half logistic distribution. Int J Appl Eng Res. 2018; 13(12): 10627-10634.

Srinivas R, Yedlapalli P, Girija SVS. On semicircular extreme-value distribution. Int J Appl Eng Res. 2019; 14(9): 2182-2187.

Subrahmanyam PS, DattatreyaRao AV, Girija SVS. On wrapping of new Weibull Pareto distribution. Int J Adv Res Rev. 2017; 2(4): 10-20.